Classification of Choroidal Neovascularization Using Projection-Resolved Optical Coherence Tomographic Angiography

Rachel Patel,[1,2] Jie Wang,[1] J. Peter Campbell,[1] Lee Kiang,[1] Andreas Lauer,[1] Christina Flaxel,[1] Thomas Hwang,[1] Brandon Lujan,[1] David Huang,[1] Steven T. Bailey,[1] and Yali Jia[1]

[1]Casey Eye Institute, Oregon Health & Science University, Portland, Oregon, United States
[2]John A Moran Eye Center, University of Utah Health, Salt Lake City, Utah, United States

PURPOSE. To evaluate if projection-resolved optical coherence tomographic angiography (PR-OCTA) reduces projection artifact with less attenuation of choroidal neovascularization (CNV) flow signal compared to conventional OCTA with slab subtraction.

METHODS. In this retrospective cross-sectional study, participants with subfoveal treatment-naïve CNV secondary to age-related macular degeneration underwent OCTA. Scans were exported for custom processing including manual segmentation as necessary, application of slab subtraction and PR-OCTA algorithm, and calculation of CNV vascular area and connectivity. CNV was classified as type 1, minimally type 2, or predominantly type 2 based on fluorescein angiography (FA) and OCT. Two masked retina specialists independently classified CNV using cross-sectional conventional OCTA and PR-OCTA.

RESULTS. A total of 17 eyes were enrolled in this study. Mean CNV vessel area (mm^2) was 0.67 ± 0.51 for PR-OCTA and 0.53 ± 0.41 for slab subtraction ($P = 0.018$). Mean vascular connectivity was 96.80 ± 1.28 for PR-OCTA and 90.90 ± 4.42 ($P = 0.018$) for slab subtraction. Within-visit repeatability (coefficient of variation) of PR-OCTA was 0.044 for CNV vessel area and 0.012 for vascular connectivity, compared to 0.093 and 0.028 by slab subtraction. PR-OCTA classification agreement with FA/OCT was 88.2% and 76.5% for the two graders, while conventional OCTA agreement was 58.8% and 70.6% (grader 1, $P = 0.025$; grader 2, $P = 0.56$). Moreover, PR-OCTA enabled the individual quantification of type 1 and type 2 components of a CNV.

CONCLUSIONS. PR-OCTA had greater CNV vessel area and vascular connectivity, as well as better repeatability, compared to slab subtraction, suggesting PR-OCTA is a superior technique for imaging CNV. Furthermore, PR-OCTA removes projection artifact on cross-sectional OCTA, improving the ability to classify and quantify CNV components.

Keywords: projection-resolved optical coherence tomographic angiography, OCTA, choroidal neovascularization, age-related macular degeneration

The advent of optical coherence tomographic angiography (OCTA) has permitted the rapid, noninvasive, and quantitative assessment of the ocular vasculature.[1] Unlike conventional fluorescein angiography (FA), OCTA provides three-dimensional (3D) visualization of the retinal vasculature. Angiographic information can be overlaid on structural optical coherence tomography (OCT) for better understanding the relations between retinal tissue and retinal and choroidal blood perfusion. However, a significant drawback to OCTA lies in the presence of flow projection artifact.[2] As the infrared beam penetrates the retina from the inner aspect, moving blood cells in the more superficial layers cast time-varying shadows on deeper layers, where they can be mistakenly interpreted as blood flow. Notably, in cases of neovascular age-related macular degeneration (AMD), projection from inner retinal vessels casts misleading artifact both above and below the RPE; this artifact interferes with the visualization of choroidal neovascularization (CNV) by en face OCTA. Additionally, projection artifact impairs the depth localization of CNV with respect to retinal structures on cross-sectional OCTA, potentially confounding characterization using histologic description as type 1 (below the RPE) or type 2 (extending within the subretinal space).

Initial efforts to mitigate the role of projection artifact on CNV detection and quantification utilized a masking technique.[3] In this method, large vessels in the en face superficial retinal slab are identified and used to generate a negative filter that is applied to the en face outer retinal and choriocapillaris slabs. This method effectively blocks the larger vessel projection artifact, but also removes flow signal from blood vessels in the outer retinal slab. A recently developed improvement in projection artifact removal, the slab-subtraction technique,[4,5] does not rely on masking vessel projections, but rather subtracts flow signal from superficial vessels from flow signal detected in the deeper layers of the retina. Compared to the masking algorithm, slab-subtraction can better retain CNV integrity, but has been shown to attenuate the flow signal of CNV.[6] An additional disadvantage of these techniques is that they are solely

applicable to en face OCTA images and do not improve the ability to discriminate CNV from projection artifact on cross-sectional OCTA.

Recently, an algorithm for projection-resolved OCTA (PR-OCTA) has been developed, clarifying the ambiguity between in situ flow and projection artifact at the level of single voxels.[7,8] This method is based on the observation that normalized projection artifact signal does not exceed the value of the original, more superficial signal. In contrast to previous methods to minimize projection artifact, including the masking algorithm or slab-subtraction techniques, PR-OCTA is applicable at the level of individual voxels and therefore equally suitable for cross-sectional scans. Such representations allow angiographic information to be superimposed with the cross-sectional OCT that is often used clinically to assess CNV.

This retrospective, cross-sectional study explores the potential advantages of PR-OCTA in evaluating CNV secondary to AMD. First, we compare the PR-OCTA method to the slab subtraction technique for quantitative CNV analysis using en face OCTA. Second, we compare PR-OCTA to conventional OCTA methods for the ability to appropriately classify CNV as pure type 1, predominantly type 2, or minimally type 2 using cross-sectional OCTA. The current standard of classifying CNV type is a multimodal imaging approach that utilizes both FA and structural OCT.[9] Because structural OCT is inherently part of OCTA scans, we compared structural OCT alone as an alternative method of classifying CNV to determine if OCTA conferred an additional advantage.

METHODS

This study was conducted with the informed consent of participants, in accordance with the tenets of the Declaration of Helsinki, and with approval of the Oregon Health & Science University institutional review board. Patients were recruited from the Retina department at Oregon Health & Science University. Inclusion criteria required treatment-naïve neovascular AMD with CNV confirmed by FA and structural OCT. Exclusion criteria were the presence of prominent media opacity or poor OCTA image quality with signal strength index less than 55. This study focused on type 1 and type 2 CNV, while cases of type 3 CNV or retinal angiomatous proliferation were excluded. CNV was then classified (STB) using traditional multimodal imaging as follows: (1) pure type 1 CNV: entire lesion was occult based on FA with corresponding elevation of RPE above Bruch's membrane (BM) on structural OCT; (2) predominantly type 2 CNV: greater than 50% of the lesion was classic on FA with corresponding subretinal hyperreflective material present on structural OCT; (3) minimally type 2: less than 50% of the lesion was classic by FA with confirmed elevation of RPE above BM in the region of occult CNV.

OCTA Acquisition and Processing

OCTA scans were acquired using commercial equipment (RTVue-XR Avanti with AngioVue; Optovue, Inc., Fremont, CA, USA) with a center wavelength of 840 nm and 70 kHz axial scan rate. A 3×3 mm or 6×6 mm area was obtained to capture the entire CNV. The CNV of each eye was captured twice to assess repeatability. Each volumetric data set consisted of two orthogonal scans. A total of 304 A-scans along the fast transverse direction were sampled, with two consecutive B-scans at each of 304 locations along the slow transverse direction. Application of the split-spectrum amplitude-decorrelation angiography algorithm detected flow as decorrelation between the two B-scans,[10,11] and registration of the two

orthogonal scans removed motion artifact. Each volumetric data set was segmented by a semiautomatic algorithm[6] to delineate the inner retinal layer (from the internal limiting membrane to the outer boundary of the outer plexiform layer [OPL]), the outer retinal layer (from the outer OPL to BM), and choroidal flow (below BM).

To generate data sets with reduced projection artifact, the PR algorithm was applied to the scans prior to segmentation, while the slab subtraction algorithm was applied afterward. The PR-OCTA algorithm identifies voxels with in situ flow as those where reflectance-normalized decorrelation values are higher than all shallower voxels in the same axial scan line. It retains flow signal from true blood vessels while suppressing projected flow signal along each axial line in deeper layers, which appears as downward tails on cross-sectional angiograms and duplicated vascular patterns on en face angiograms.[7] To apply the slab subtraction algorithm, the inner retinal angiogram was filtered, multiplied by a scaling factor of 1.1, and then subtracted from the outer retinal angiogram.

Quantification of CNV Vascular Area and Vascular Connectivity

On each outer retinal en face slab of PR-OCTA or slab subtraction OCTA, the CNV membrane area was automatically detected by a saliency model (Fig. 1).[4,12] Otsu's method was applied to search for a threshold that maximized interclass variation and distinguished CNV flow signal from the isolated background speckle noise.

The CNV vascular area was determined with each projection removal method and the capability to preserve the CNV flow signal was compared. CNV vascular area was calculated by multiplying the pixel size by the number of pixels containing CNV flow. CNV vascular connectivity by each method was determined by first detecting vascular skeletons (lines with the width of a single pixel) on CNV binary images. Vascular connectivity was calculated as the ratio of the number of connected skeleton pixels to the total number of skeletonized pixels. To be included as connected pixels, a minimum number of 5 pixels were required. Repeatability of the CNV area and vessel connectivity was determined by calculating the coefficient of variation (CV) of the 2 scans of each eye. A value of $P = 0.05$ was used to establish statistical significance.

Classification of Choroidal Neovascularization

Two retina specialists (JPC, LK) were trained as graders to use cross-sectional OCTA to classify CNV as pure type 1, predominantly type 2, or minimally type 2 using examples of CNV that were not included in this study. Each grader was masked to traditional classification based on multimodal imaging. First, each grader reviewed the entire volumetric angiogram of the structural OCT, classifying each case of CNV. For grading cross-sectional OCTA, each grader could review the entire volumetric data set as well as an en face image of the outer retinal slab to help localize the CNV. The graders first evaluated standard cross-sectional OCTA with projection artifact followed by cross-sectional PR-OCTA. McNemar's test was applied to compare the number of accurate responses by PR-OCTA to those by conventional OCTA for each grader. Given the sample size, no subdivision analysis based on CNV type was performed. All statistical analyses were performed with commercial software (SPSS 20.0; SPSS, Inc., Chicago, IL, USA, and MedCalc 10.1.3.0; MedCalc Software, Ostend, Belgium, www.medcalc.be).
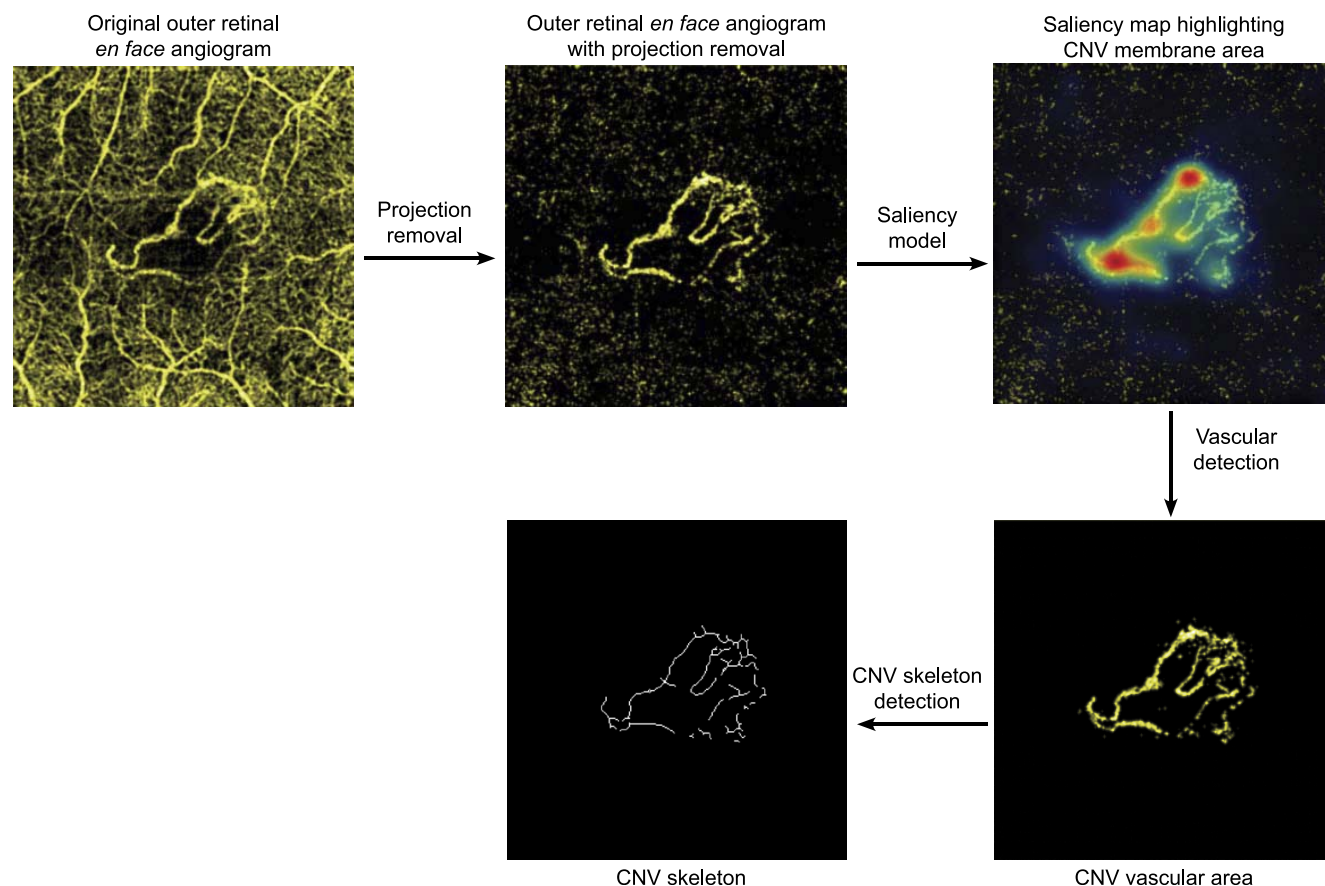
FIGURE 1. Method of determining CNV area and skeleton. Illustrative steps of generating the CNV vascular area and skeleton from the original outer retinal en face OCTA image using a saliency model.

RESULTS

In total, 22 eyes of 22 patients with treatment-naïve neovascular AMD were enrolled. Five eyes were excluded due to poor image quality (signal strength index less than 55) and 17 were used for grader classification (11 women). Ten of these 17 eyes had 2 scans within the same visit and were thus used to calculate repeatability. The mean age of the 17 patients in this analysis was 71.9 ± 8.8 years and mean logMAR visual acuity was 0.30 ± 0.2. Using traditional multimodal imaging, 10 eyes were classified as having pure type 1 CNV, 5 as predominantly type 2 CNV, and 2 as minimally type 2 CNV. In all cases, the entire CNV was present in the 3×3 mm or 6×6 mm OCTA scanning area.

Quantification of CNV Vascular Area and Vascular Connectivity

The quantitative assessment of CNV cases is summarized in Table 1. PR-OCTA had significantly greater CNV vascular area and vascular connectivity compared to slab subtraction. Additionally, PR-OCTA had better within-visit repeatability for both CNV vascular area and vascular connectivity compared to slab subtraction technique.

Figure 2 illustrates examples of types of CNV under original OCTA, slab subtraction, and PR-OCTA. Notably, slab subtraction technique resulted in attenuated CNV signal and smaller CNV vessel areas compared to PR-OCTA. By necessity, the cross-sectional angiography scans represented in the slab subtraction column are unchanged from the original OCTA,

as the slab subtraction algorithm cannot be applied to cross-sectional scans.

Classification of Choroidal Neovascularization

PR-OCTA had the best agreement with traditional multimodal imaging in classifying CNV type, followed by conventional OCTA and then structural OCT alone. A summary of the graders' classifications is presented in Table 2. For both graders, PR-OCTA but not OCTA significantly improved discrimination compared to structural OCT (grader 1, $P = 0.034$; grader 2, $P = 0.025$). PR-OCTA also improved classification compared to OCTA for grader 1 ($P = 0.025$) but not grader 2 ($P = 0.56$). The accuracy of either grader in identifying a particular classification category was not statistically significant between OCTA and PR-OCTA. Given the small selection of cases, intragrader agreement was not assessed.

Figure 2 demonstrates examples of en face OCTA and cross-sectional OCTA and PR-OCTA that the graders used for classification, including cases with pure type 1, minimally type 2, and predominantly type 2 CNV. (The slab subtraction images were not used for classification given that the algorithm cannot be applied to cross-sectional images.) In a case of pure type 1 CNV (Fig. 2, top 2 rows), the original cross-sectional OCTA illustrated streaks of neovascular signal above the RPE, while projection resolution revealed the CNV to be limited to the sub-RPE space. In a case of predominantly type 2 CNV (Fig. 2, bottom 2 rows), projection resolution diminished angiographic signal below the RPE but preserved that above it. In this case, both graders inaccurately classified the original OCTA scan as

TABLE 1. Comparative Vascular Connectivity and Vascular Area

	CNV Vascular Area, mm^2	CNV Vascular Connectivity	CV of CNV Vascular Area	CV of CNV Vascular Connectivity
Slab subtraction	0.53 ± 0.41	90.90 ± 4.42	0.093	0.028
PR-OCTA	0.67 ± 0.51	96.80 ± 1.28	0.044	0.012
Improvement, %	26.4	6.49		
P value	0.018	0.018		

All 17 eyes were employed for analysis of vascular area and connectivity, represented as mean ± standard deviation. A paired *t*-test was used to calculate the *P* value. CV was calculated using the 10 cases for which 2 within-visit scans were available.

minimally type 2, but with PR-OCTA accurately determined the majority of the CNV was above the RPE, and thereby type 2.

In cases containing both type 1 and type 2 components of CNV, application of the PR-OCTA algorithm along with segmentation along the RPE enabled the generation of two en face OCTA images corresponding to individual representation of type 1 and type 2 components (Fig. 3). Generating distinct images permitted quantification of the vascular area of each component.

In a case of predominantly type 2 CNV based on FA (Fig. 3, top 2 rows), the quantified area of the type 2 component exceeded that of the type 1 component. In case 2 (Fig. 3, bottom 2 rows), the FA contained 2 small areas of early hyperfluorescence (red circle) consistent with a classic component of CNV. In the later frames, an adjacent area of leakage and staining is evidenced consistent with the development of a fibrovascular pigment epithelial detachment; this lesion was characterized as minimally type 2 with FA/OCT. The PR-OCTA images revealed a larger than expected type 2 component that was difficult to see with FA because a region of dense hyperreflective material (visible on structural OCT) likely obscured vessels between the hyperreflective material and the RPE. With PR-OCTA, there was definitive flow signal within this region. This second case is an example in which PR-OCTA and FA/OCT disagree in classification and illustrates one of the relative advantages of PR-OCTA.

DISCUSSION

Over the last several years, clinicians have embraced emerging OCTA technologies in part because of novel visualization of CNV vascular structures. Several studies have shown the sensitivity and specificity of CNV detection with OCTA approach that of the traditional method of FA.[13-15] However, the inherent projection artifact of OCTA imaging obscures en face visualization of CNV and interferes with CNV quantification. Prior methods to remove projection artifact may attenuate CNV signal on en face OCTA. The PR-OCTA technique tested in this study removed projection artifact with improved en face CNV vascular connectivity and better within-visit repeatability compared to slab subtraction. Additionally, the CNV vessel area was greater with PR-OCTA, suggesting that the PR algorithm suppressed projection artifact with less attenuation of CNV signal compared to slab subtraction (Fig. 2).

Traditional angiography with fluorescein dye utilizes specific leakage patterns such as occult and classic to characterize lesion types. These patterns were useful for guiding laser-based therapy in the past. In contrast Gass devised a histology-derived classification, identifying CNV

between BM and the RPE as type 1, and CNV that extended above the RPE into the subretinal space as type 2.[16] Freund demonstrated that multimodal imaging combining FA with spectral domain OCT has potential to differentiate the categories of CNV[17] that may exhibit unique treatment response under anti-endothelial VEGF treatment.[18,19]

Because cross-sectional OCTA provides simultaneous depth resolved flow information and its relationship to retinal anatomic structure, several studies have classified CNV as type 1 or type 2 using this technique.[3,20] However, to date, no study has compared OCTA classification to multimodal imaging or to structural OCT alone. Additionally, no study has attempted to evaluate how projection artifact affects the classification. In this study (Table 2), structural OCT only agreed with traditional FA/OCT in approximately half of the cases. Interestingly, OCTA with slab subtraction technique agreed with FA/OCT in lesion type in 58.8% and 70% of cases for the two graders and was statistically not superior to structural OCT alone. The application of PR-OCTA had closest agreement with FA/OCT, with significantly better agreement compared to structural OCT for both graders and better agreement compared to traditional OCTA for one of the two graders. It is not surprising that FA/OCT does not always agree with PR-OCTA in classifying CNV. With FA, leakage patterns of different components may overlap, impairing the ability to discriminate CNV types or leakage patterns, and thus interfering with assessment and classification (Fig. 3, case 2).

This study included 10 cases of pure type 1 CNV, 5 of minimally type 2 CNV, and 2 of predominantly type 2 CNV. Although the number of cases within each classification is limited, our results suggested that the application of PR-OCTA most improved the detection of minimally type 2 CNV. This trend may be due in part to the difficulty inherent in classifying CNV with strong flow signals both above and below the RPE. Moreover, graders were less likely to incorrectly classify scans as predominantly type 2 using PR-OCTA, which may be attributed to the removal of projected signal from retinal vessels into the outer retina. Of note, in the few cases with moderately low signal strength index, projection artifacts were suppressed but not entirely removed from the RPE and subretinal hyperreflective material, likely contributing to grader misclassification.

The slab subtraction technique does not remove projection artifact originating from the superficial components of CNV that project onto deeper structures. Because PR-OCTA addresses artifact on a voxel by voxel basis throughout the entire 3D volume and is not limited to superficial retinal vessels, it can mitigate the projection artifact from both overlying retinal vessels as well as from the more inner portions of the CNV improving depth resolution and the ability to classify CNV.

Because projection artifact of inner portion of CNV can be mitigated, separate quantification of type 1 CNV and type 2 CNV components with a lesion is now possible (Fig. 3). This technique is dependent on accurate segmentation along the RPE. While in most cross-sectional scans segmentation is straightforward, in some scans underlying pathology associated with AMD such as RPE atrophy or subretinal hyperreflective material make the RPE indistinguishable from surrounding tissue. In these instances, RPE segmentation is estimated. Several studies have demonstrated quantitative OCTA-derived CNV metrics,[21-23] which may decrease after anti-VEGF treatment or increase when treatment is suspended. However, the role of OCTA CNV biomarkers in routine anti-VEGF management decisions has not yet been defined. With improving OCTA technology such as application of PR-OCTA, refined quantitative CNV metrics have the potential to function as a more clinically useful biomarker with which to assess the
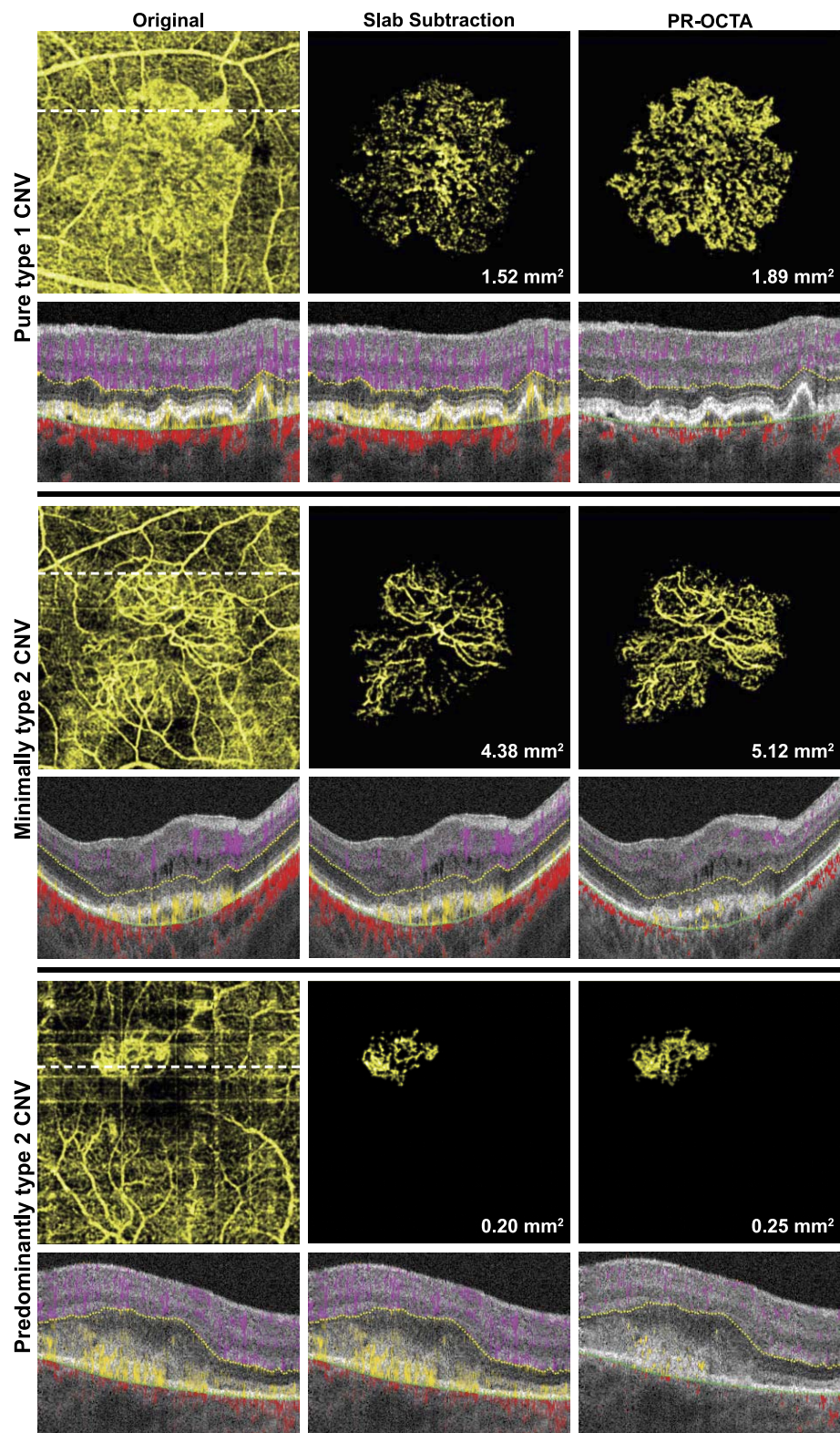
FIGURE 2. Three types of CNV. Illustrative examples of pure type 1, minimally type 2, and predominantly type 2 CNV by original, slab subtraction, and PR-OCTA. Numbers reflect calculated CNV vascular areas. The scans of minimally type 2 CNV are 6×6 mm while the others are 3×3 mm.

natural history of CNV and treatment response. Previous investigation suggests type 2 CNV is more responsive to anti-VEGF treatment compared to type 1 CNV.[24] Now for the first time, individual quantified CNV components response to treatment can be studied.

This investigation was limited by the number of eyes that were enrolled, as well as by the variety of types of CNV, which precluded further assessment of intragrader agreement. Graders saw each CNV three times (by OCT, OCTA, and PR-OCTA), which may have facilitated the more accurate grading

TABLE 2. Agreement of CNV Classification as Type 1, Predominantly Type 2, or Minimally Type 2

| | Agreement of CNV Type With Respect to FA/OCT, *n*/Total (%) | | | Differentiation Between Agreement Percentages (McNemar's Test), *P* Value | | |
	OCT	OCTA	PR-OCTA	OCT vs. OCTA	OCT vs. PR-OCTA	OCTA vs. PR-OCTA
Grader 1	9/17 (52.9)	10/17 (58.8)	15/17 (88.2)	0.74	0.034	0.025
Grader 2	7/17 (41.2)	12/17 (70.6)	13/17 (76.5)	0.10	0.025	0.56

of subsequent images seen. Moreover, while each CNV included in this study was fully captured by the region scanned by OCTA, scanning areas larger than 6×6 mm are desirable for future clinical practice.

In summary, PR-OCTA addresses projection artifact within both en face and cross-sectional angiographic images, and is better able to preserve in situ CNV compared to older projection artifact removal techniques. Additionally, PR-OCTA
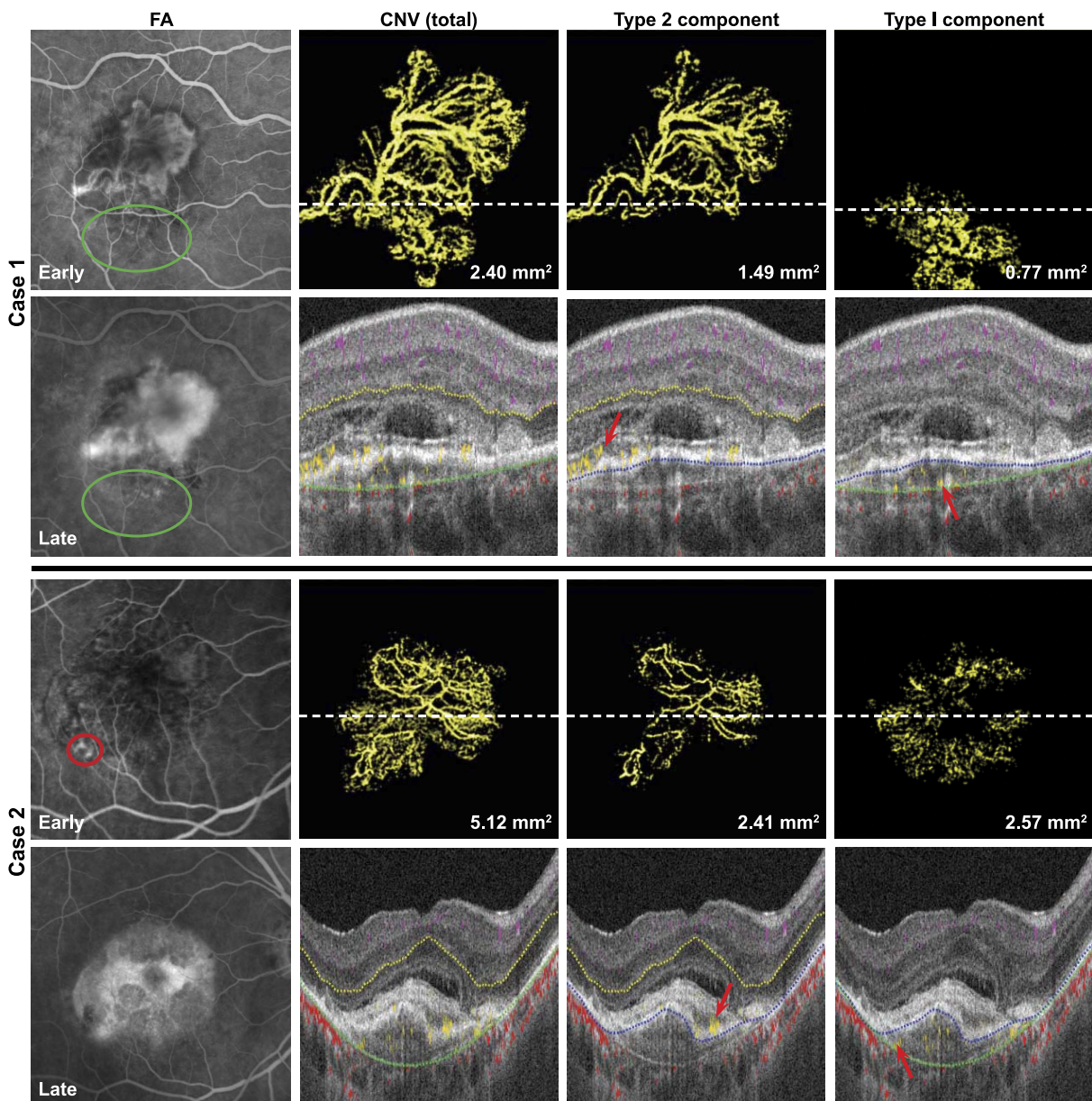

FIGURE 3. Distinction of type 1 and type 2 components of CNV. Two cases of CNV containing both type 1 and type 2 components. *White lines* correlate to the cross-sectional scan pictured below, and numbers correspond to CNV vascular areas. *Red arrows* highlight regions containing CNV. In case 1, *green ovals* indicate the region of occult CNV by FA and in case 2 the *red circle* marks the regions of early hyperfluorescence indicative of a classic component of CNV. Case 1 employs a 3×3 mm OCTA scan, and case 2 a 6×6 mm scan.

allows for the individual calculation of CNV vessel areas for type 1 and type 2 CNV without the projection artifact of type 2 CNV affecting CNV vessel area measurement of the type 1 component. Longitudinal studies using PR-OCTA are needed to validate the clinical utility of CNV biomarkers.

References

1. Jia Y, Bailey ST, Hwang TS, et al. Quantitative optical coherence tomography angiography of vascular abnormalities in the living human eye. *Proc Natl Acad Sci U S A*. 2015;112: E2395–E2402.

2. Gao SS, Jia Y, Huang D. Artifacts. In: Huang D, Lumbroso B, Jia Y, Waheed NK, eds. *Optical Coherence Tomography Angiography of the Eye*. Thorofare, NJ: SLACK Inc.; 2017.

3. Jia Y, Bailey ST, Wilson DJ, et al. Quantitative optical coherence tomography angiography of choroidal neovascularization in age-related macular degeneration. *Ophthalmology*. 2014;121:1435–1444.

4. Liu L, Gao SS, Bailey ST, Huang D, Li D, Jia Y. Automated choroidal neovascularization detection algorithm for optical coherence tomography angiography. *Biomed Opt Express*. 2015;6:3564–3576.

5. Zhang A, Zhang Q, Wang RK. Minimizing projection artifacts for accurate presentation of choroidal neovascularization in OCT micro-angiography. *Biomed Opt Express*. 2015;6:4130–4143.

6. Zhang M, Wang J, Pechauer AD, et al. Advanced image processing for optical coherence tomographic angiography of macular diseases. *Biomed Opt Express*. 2015;6:4661–4675.

7. Zhang M, Hwang TS, Campbell JP, et al. Projection-resolved optical coherence tomographic angiography. *Biomed Opt Express*. 2016;7:816–828.

8. Wang J, Zhang M, Hwang TS, et al. Reflectance-based projection-resolved optical coherence tomography angiography. *Biomed Opt Express*. 2017;8:1536–1548.

9. Freund KB, Zweifel SA, Engelbert M. Do we need a new classification for choroidal neovascularization in age-related macular degeneration? *Retina*. 2010;30:1333–1349.

10. Jia Y, Tan O, Tokayer J, et al. Split-spectrum amplitude-decorrelation angiography with optical coherence tomography. *Opt Express*. 2012;20:4710–4725.

11. Gao SS, Liu G, Huang D, Jia Y. Optimization of the split-spectrum amplitude-decorrelation angiography algorithm on a spectral optical coherence tomography system. *Opt Lett*. 2015;40:2305–2308.

12. Gao SS, Liu L, Bailey ST, et al. Quantification of choroidal neovascularization vessel length using optical coherence tomography angiography. *J Biomed Opt*. 2016;21:76010.

13. de Carlo TE, Bonini Filho MA, Chin AT, et al. Spectral-domain optical coherence tomography angiography of choroidal neovascularization. *Ophthalmology*. 2015;122:1228–1238.

14. Carnevali A, Cicinelli MV, Capuano V, et al. Optical coherence tomography angiography: a useful tool for diagnosis of treatment-naive quiescent choroidal neovascularization. *Am J Ophthalmol*. 2016;169:189–198.

15. Faridi A, Jia Y, Gao SS, et al. Sensitivity and specificity of OCT angiography to detect choroidal neovascularization. *Ophthalmol Retina*. 2017;1:294–303.

16. Gass JD. Biomicroscopic and histopathologic considerations regarding the feasibility of surgical excision of subfoveal neovascular membranes. *Am J Ophthalmol*. 1994;118:285–298.

17. Freund KB, Zweifel SA, Engelbert M. Do we need a new classification for choroidal neovascularization in age-related macular degeneration? *Retina*. 2010;30:1333–1349.

18. Brown DM, Kaiser PK, Michels M, et al. Ranibizumab versus verteporfin for neovascular age-related macular degeneration. *N Engl J Med*. 2006;355:1432–1444.

19. Rosenfeld PJ, Brown DM, Heier JS, et al. Ranibizumab for neovascular age-related macular degeneration. *N Engl J Med*. 2006;355:1419–1431.

20. Malihi M, Jia Y, Gao SS, et al. Optical coherence tomographic angiography of choroidal neovascularization ill-defined with fluorescein angiography. *Br J Ophthalmol*. 2017;101:45–50.

21. Huang D, Jia Y, Rispoli M, Tan O, Lumbroso B. Optical coherence tomography angiography of time course of choroidal neovascularization in response to anti-angiogenic treatment. *Retina*. 2015;35:2260–2264.

22. Muakkassa NW, Chin AT, de Carlo T, et al. Characterizing the effect of anti-vascular endothelial growth factor therapy on treatment-naive choroidal neovascularization using optical coherence tomography angiography. *Retina*. 2015;35:2252–2259.

23. Al-Sheikh M, Iafe NA, Phasukkijwatana N, Sadda SR, Sarraf D. Biomarkers of neovascular activity in age-related macular degeneration using optical coherence tomography angiography. *Retina*. 2018;38:220–230.

24. Ying GS, Huang J, Maguire MG, et al. Baseline predictors for one-year visual outcomes with ranibizumab or bevacizumab for neovascular age-related macular degeneration. *Ophthalmology*. 2013;120:122–129.